Electronic Supplementary Material (ESI) for Dalton Transactions.

Supporting Information

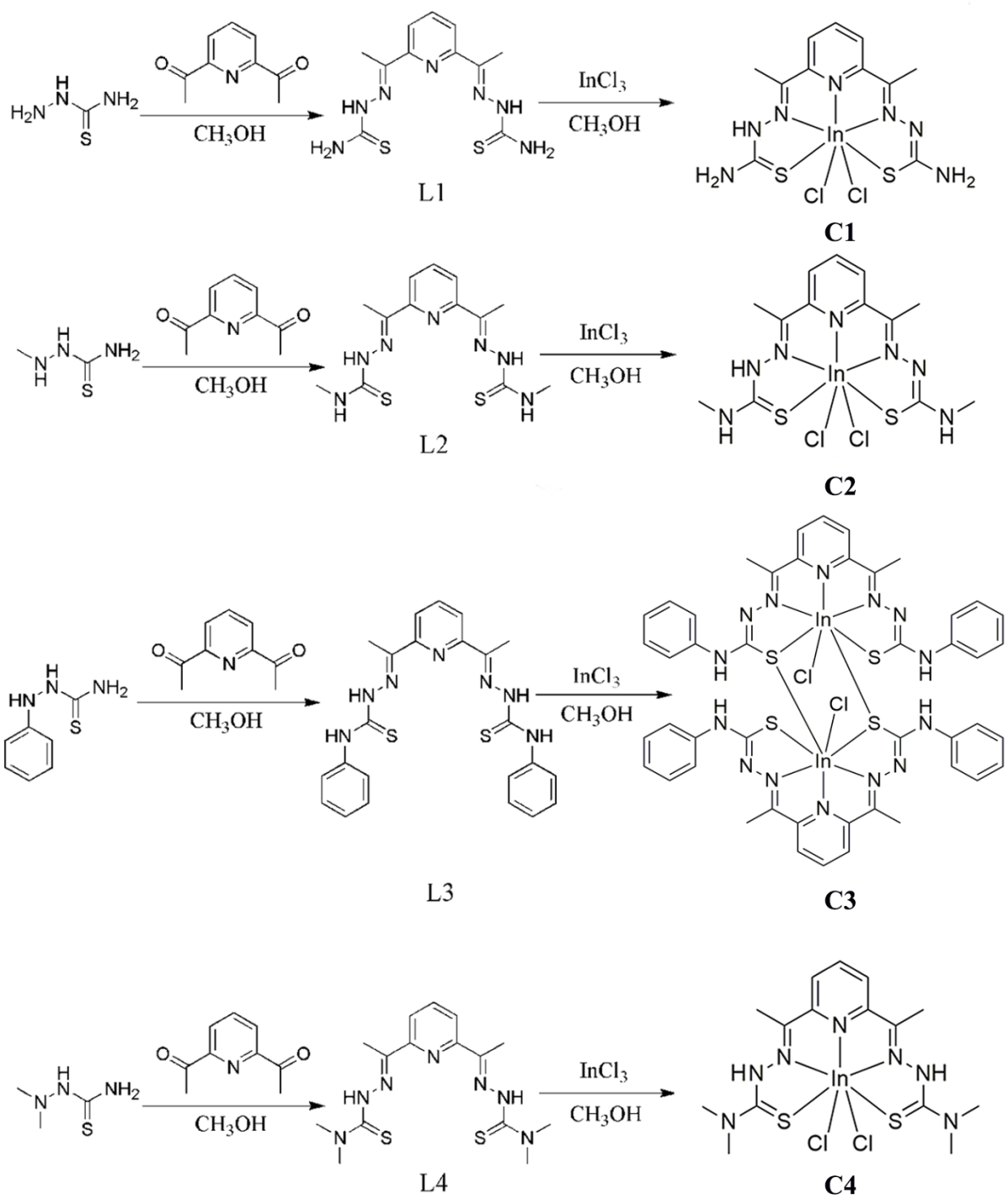

Scheme 1 Synthetic route of In(III) complexes (C1-C4)

Table S1 Bond lengths (Å) of four In(III) complexes

	C1	**C2**	**C3**	**C4**
In1-Cl1	2.4996(8)	2.578(2)	2.4660(6)	2.5343(12)
In1-Cl2	2.5960(8)	2.486(2)		
In1-S1	2.5987(8)	2.5673(19)	2.7257(6)	
In1-S2	2.6296(8)	2.652(2)	2.5305(6)	
In1-N3	2.328(2)	2.348(5)	2.3634(17)	
In1-N4	2.340(2)	2.330(5)	2.3040(17)	
In1-N5	2.464(2)	2.455(5)	2.3678(18)	
In1-S1^{1}			2.8488(6)	
In1-S02				2.6001(14)
In1-S02^{1}				2.6001(14)
In1-Cl1^{1}				2.5344(12)
In1-N2				2.386(4)
In1-N2^{1}				2.386(4)
In1-N1				2.298(5)

Table S2 Bond angles ( ) of four In(III) complexes

C1			
Cl2-In1-S2	93.68(3)	N3-In1-Cl1	92.60(6)
Cl2-In1-S1	90.54(3)	N3-In1-S2	153.56(6)
Cl1-In1-Cl2	170.87(2)	N3-In1-S1	74.40(6)
Cl1-In1-S2	92.33(3)	N3-In1-N5	134.71(8)
Cl1-In1-S1	97.34(3)	N3-In1-N4	68.93(8)
S1-In1-S2	79.21(2)	N4-In1-Cl2	85.73(6)
N5-In1-Cl2	87.83(5)	N4-In1-Cl1	85.19(6)
N5-In1-Cl1	87.58(5)	N4-In1-S2	137.41(6)
N5-In1-S2	71.46(5)	N4-In1-S1	143.32(6)
N5-In1-S1	150.44(5)	N4-In1-N5	65.96(7)
N3-In1-Cl2	85.06(6)		

C2			
Cl1-In1-S2	89.44(7)	N5-In1-Cl1	88.27(11)
S1-In1-C11	91.69(6)	N5-In1-Cl2	83.98(11)
S1-In1-S2	77.64(6)	N5-In1-S2	72.08(11)
Cl2-In1-C11	170.96(5)	N5-In1-S1	149.72(12)
Cl2-In1-S1	97.33(5)	N4-In1-Cl1	85.81(11)
Cl2-In1-S2	92.58(6)	N4-In1-S1	143.54(12)
N3-In1-C11	90.56(12)	N4-In1-S2	138.56(12)
N3-In1-S1	74.47(12)	N4-In1-Cl2	86.85(11)
N3-In1-S2	152.10(12)	N4-In1-N3	69.20(16)
N3-In1-Cl2	91.76(12)	N4-In1-N5	66.66(15)
N3-In1-N5	135.81(16)		

C3			
Cl1-In1-S1	101.38(2)	N4-In1-S1	136.64(5)
Cl1-In1-S1^{1}	167.68(2)	N4-In1-S2	142.31(5)
Cl1-In1-S2	96.42(2)	N4-In1-N5	68.23(6)
S1-In1-S1^{1}	82.858(18)	N4-In1-N3	68.83(6)
S2-In1-S1^{1}	95.77(2)	N3-In1-C11	85.05(5)
S2-In1-S1	78.455(18)	N3-In1-S1	70.58(5)
N5-In1-Cl1	96.82(5)	N3-In1-S1^{1}	85.51(5)
N5-In1-S1^{1}	84.77(5)	N3-In1-S2	148.62(5)
N5-In1-S1	148.51(5)	N3-In1-N5	137.00(6)
N5-In1-S2	74.12(5)	N4-In1-S1^{1}	79.47(5)
N4-In1-Cl1	89.75(5)		

C4			
S02^{1}-In1-S02	78.87(6)	N2-In1-Cl1	91.16(9)
Cl1^{1}-In1-S02	96.51(5)	N2^{1}-In1-Cl1^{1}	91.16(9)
Cl1-In1-S02	91.05(4)	N2-In1-N2^{1}	136.3(2)
Cl1^{1}-In1-S02^{1}	91.05(4)	N1-In1-N2^{1}	68.14(10)
Cl1^{1}-In1-Cl1	170.22(6)	N1-In1-S02^{1}	140.56(3)
N2^{1}-In1-S02^{1}	72.73(10)	N1-In1-S02	140.57(3)
N2^{1}-In1-S02	150.69(10)	N1-In1-Cl1^{1}	85.11(3)
N2-In1-S02^{1}	150.69(10)	N1-In1-Cl1	85.11(3)
N2-In1-S02	72.73(10)	N1-In1-N2	68.14(10)
N2^{1}-In1-Cl1	85.19(9)	N2-In1-Cl1^{1}	85.20(9)

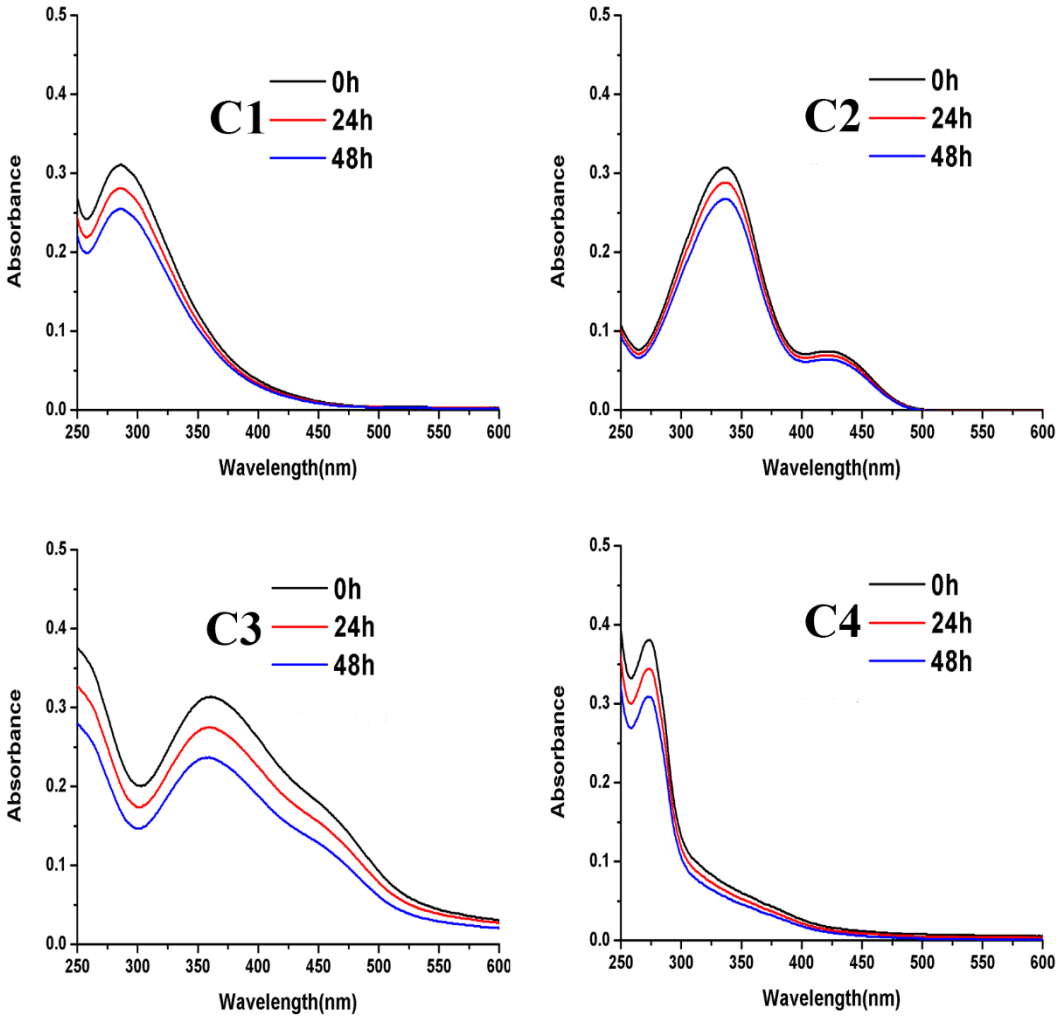

Figure S1 UV-Vis spectra of the In(III) complexes stability (C1-C4).

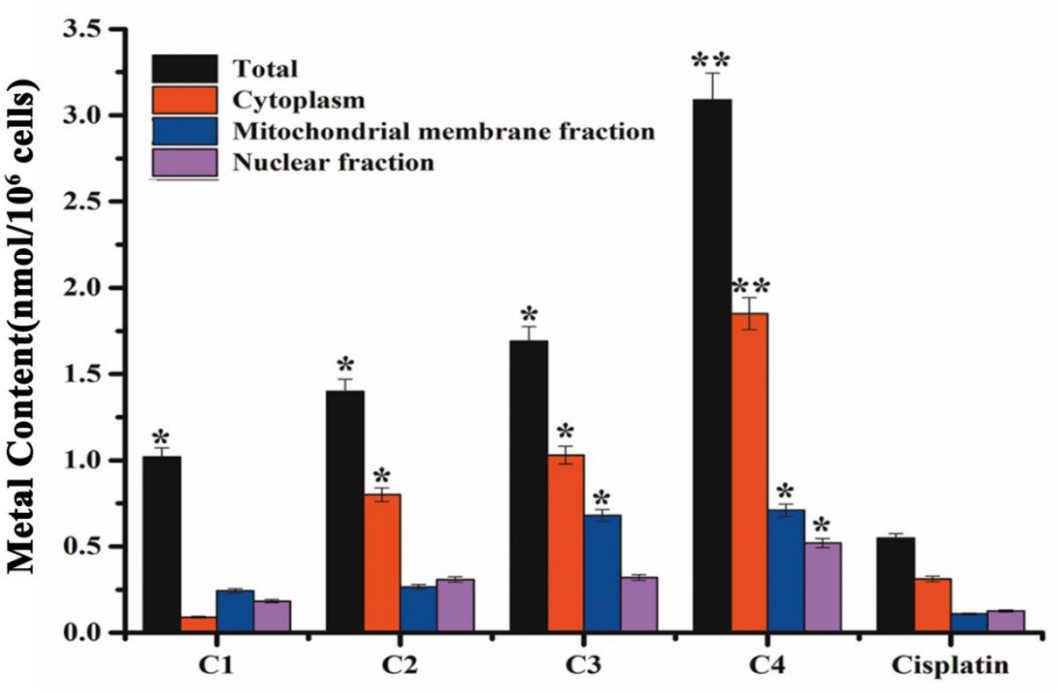

Figure S2 ICP-MS analysis of the total metal contents in the cytoplasm, mitochondria, and in the nucleus of T24 cells treated with cisplatin and C1-C4 for 24 hours; mean ± SD (n= 3): (*)$p < 0.05$, (**) $p < 0.01$.

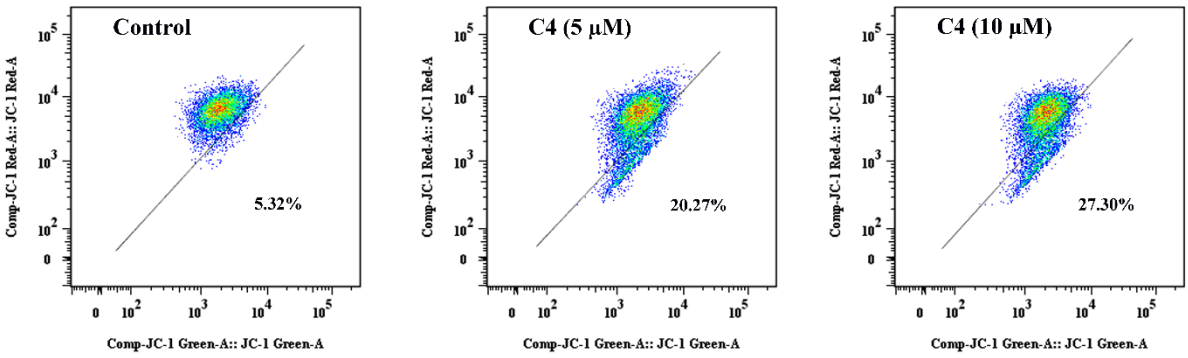

Figure S3 Assay of T24 cells mitochondrial membrane potential with JC-1 as fluorescence probe staining compare with untreated cells.

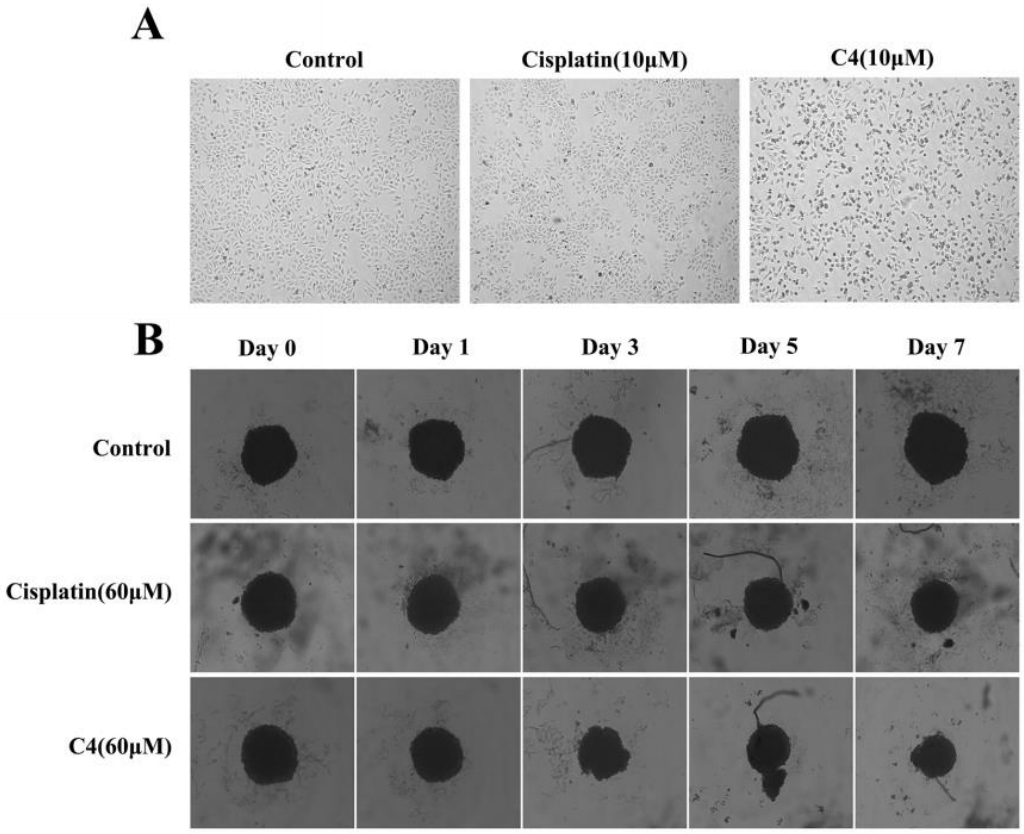

Figure S4 A analysis of cell morphology in T24 cells after treatment with C4 and Cis-platin. **B** 3D morphology of T24 cells tumor spheroids with vehicles, C4 and Cis-platin with specified concentrations for 8-days.

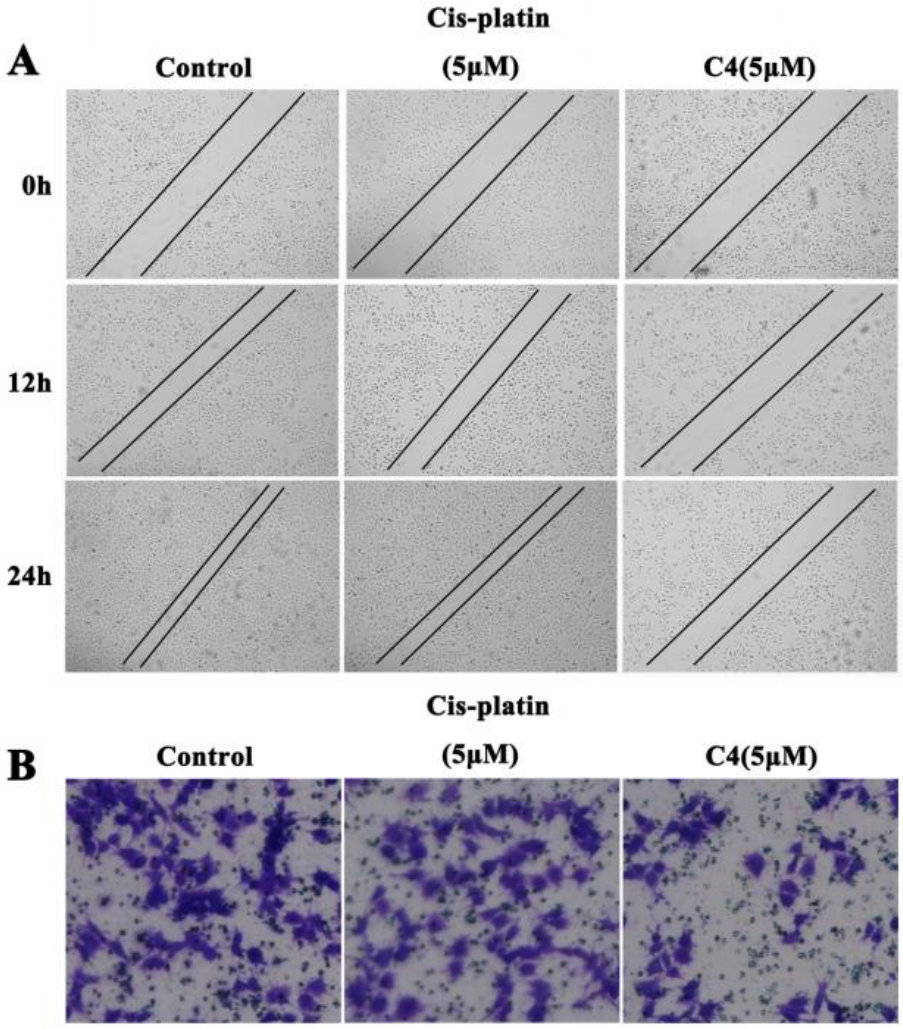

Figure S5 Analysis of the metastasis in T24 cells after treated with C4 and Cis-platin. **A** wound healing assay, during a 24-hour wound closure assay pictures were taken using a time-lapse microscope. **B** A diagram of the transwell insert apparatus used to measure cell migration and invasion cells.

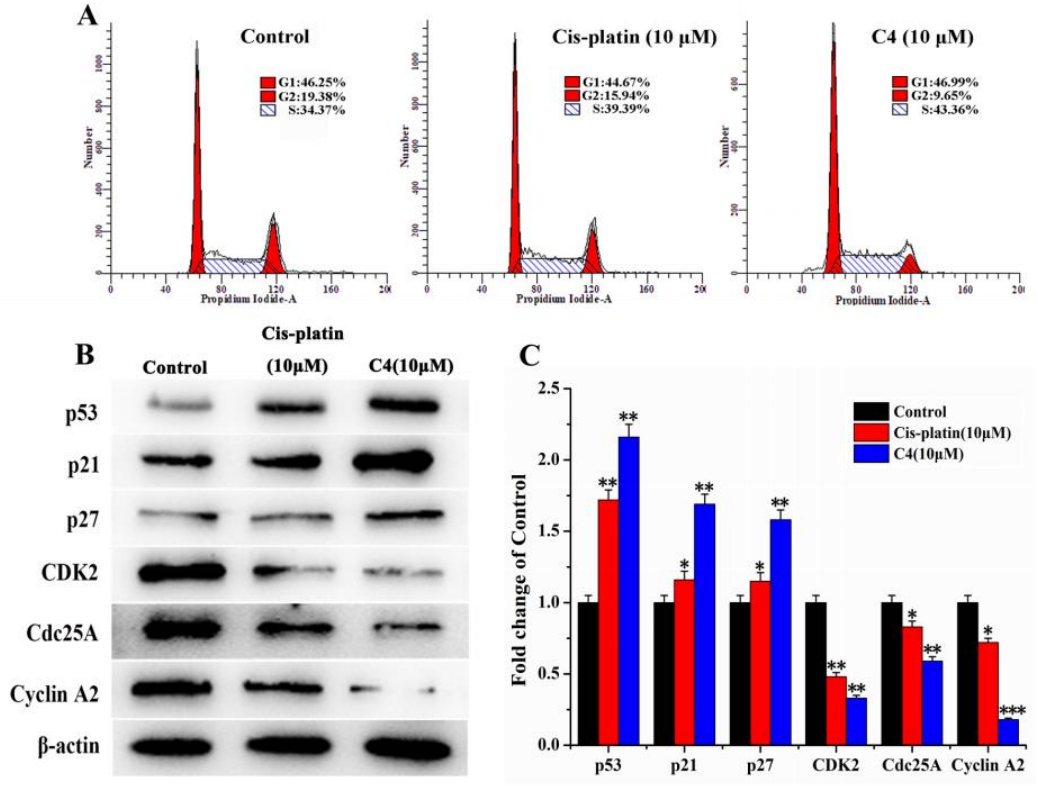

Figure S6 A Effect of the cell cycle of T24 Cells treated with C4 (10 μM) and Cis-platin(10 μM) compare with untreated cells. **B** analysis of the expression level of p53, Cdc25A, Cyclin A2, CDK2, p21, and p27. **C**. percentage expression level of p53, Cdc25A, Cyclin A2, CDK2, p21, and p27; mean ± SD (n= 3): (*)$p < 0.05$, (**) $p < 0.01$, (***) $p < 0.001$.

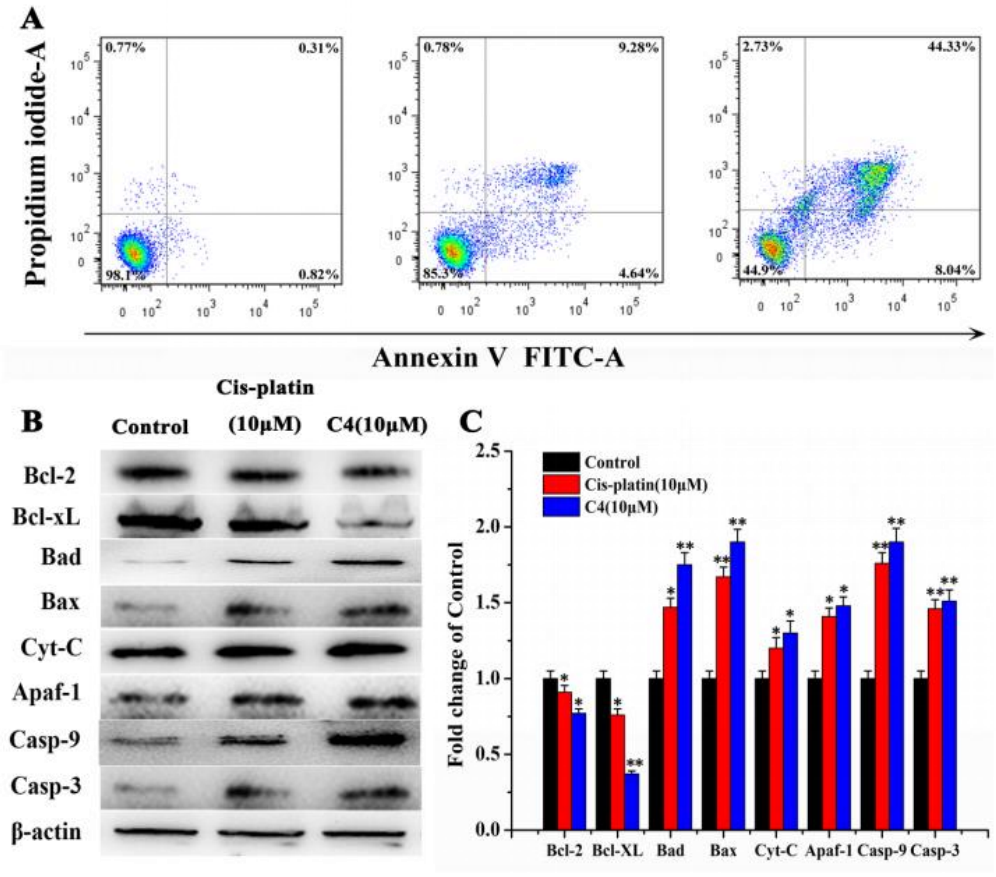

Figure S7 A Effect of cell apoptosis of T24 cells treated with C4 (10 μM) and Cis-platin(10μM) comparing with untreated cells. **B** Western blot analysis of Apaf-1, Bad, Bax, Bcl-2, Bcl-xl, and Cytochrome C, **C**. percentage expression level of Apaf-1, Bad, Bax, Bcl-2, Bcl-xl, Cytochrome C, Casp-9 and Casp-3 relative to control; mean ± SD (n= 3):(*)$p < 0.05$, (**) $p < 0.01$.

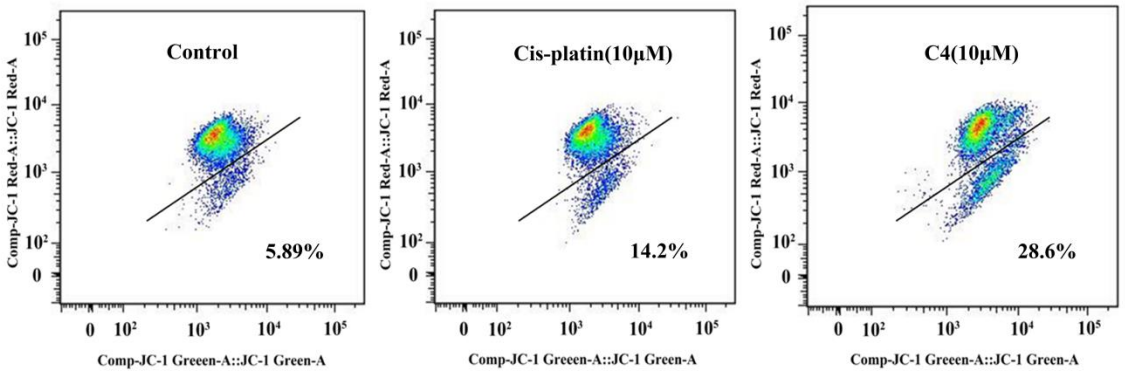

Figure S8 Assay of T24 cells mitochondrial membrane potential with JC-1 as fluorescence probe staining compare with cisplatin-treated cells.

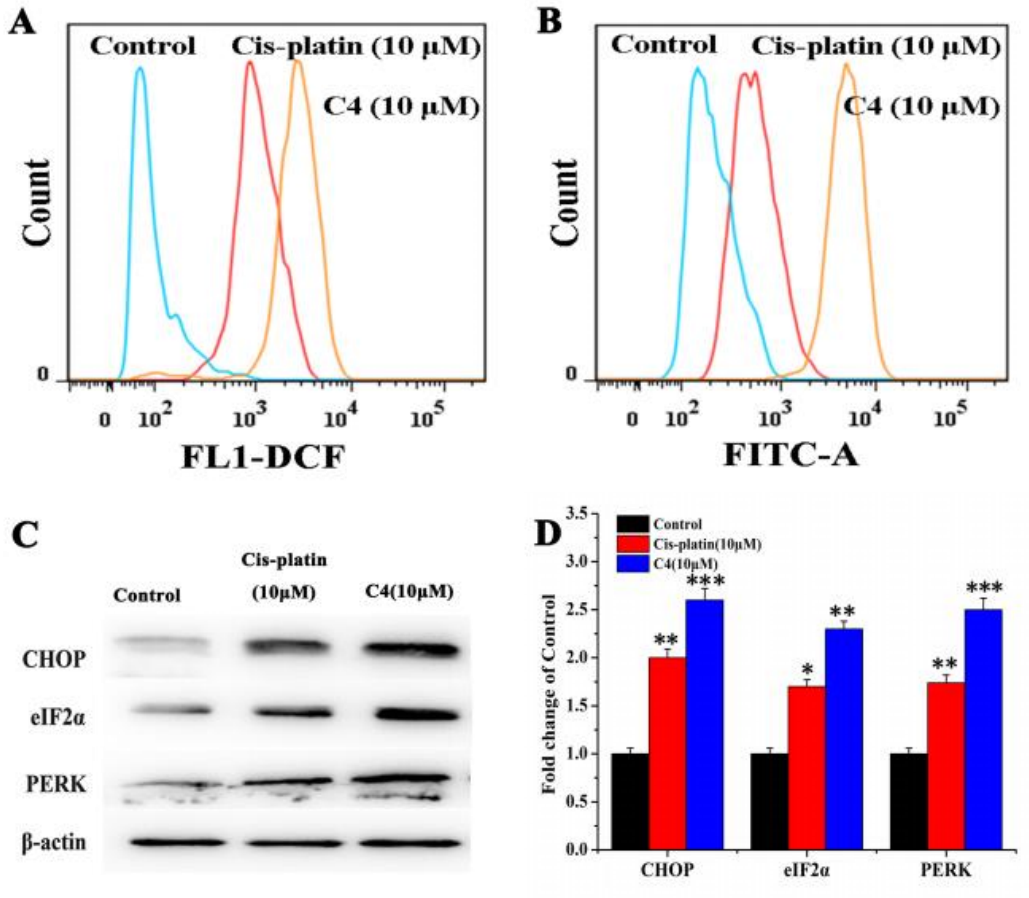

Figure S9 T24 cells treated with C4 、Cis-platin and analysis of **A** ROS concentration, **B** $Ca2^{+}$ concentration in T24 cells, **C** Western blot analysis of PERK, eIF2α and CHOP in T24 cells, **D** Graphical presentation of the expression level of PERK, eIF2α, and CHOP; mean ± SD (n= 3):(*)$p < 0.05$, (**) $p < 0.01$, (***) $p < 0.001$.

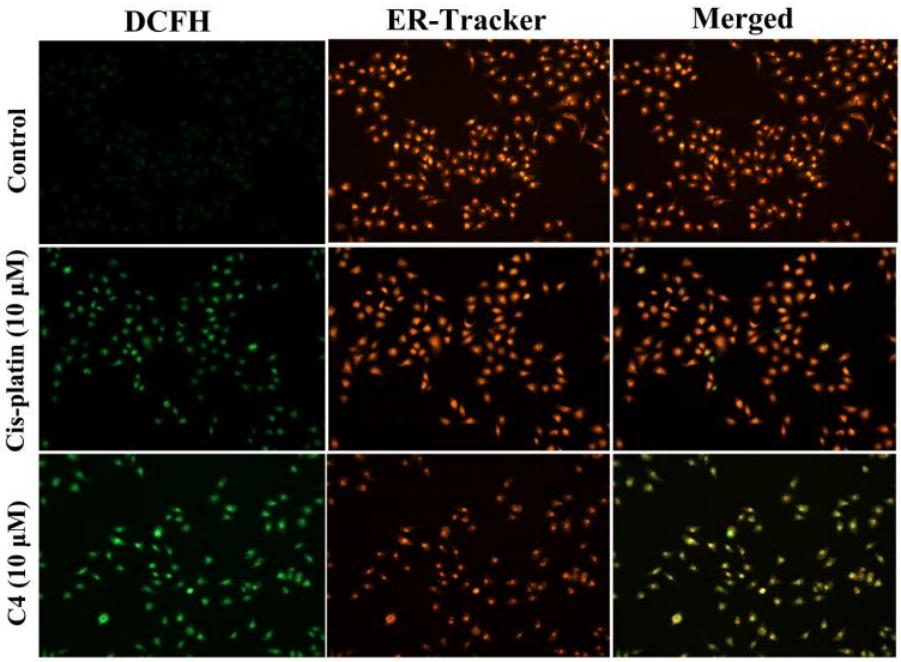

Figure S10 Generation of ROS by using 2′,7′-dichlorofluorescein (DCF) and analysis of ER-tracker red by binding to Sulfonylurea receptor in ER.

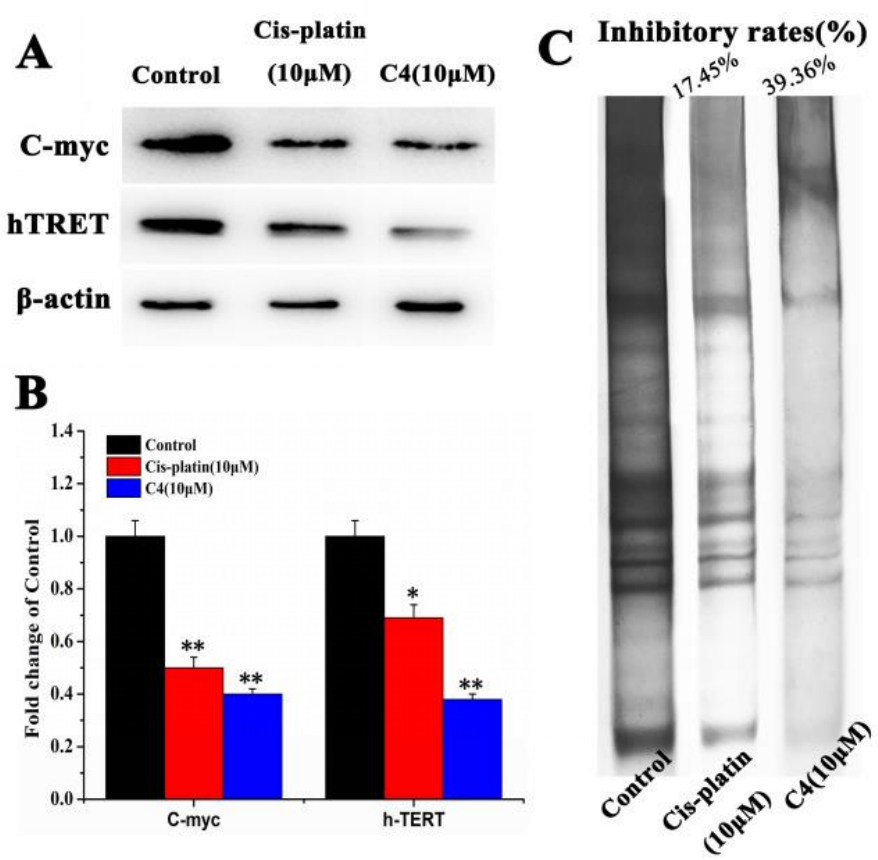

Figure S11 A Western blot analysis of c-myc and hTERT in T24 cells treated with C4 and Cis-platin for 24 h, **B** Densitometric analysis of hTERT and c-myc proteins, **C** The influence on the telomerase activity in the T24 cells treated with C4 and Cis-platin; mean ± SD (n= 3):(*)$p < 0.05$, (**) $p < 0.01$.

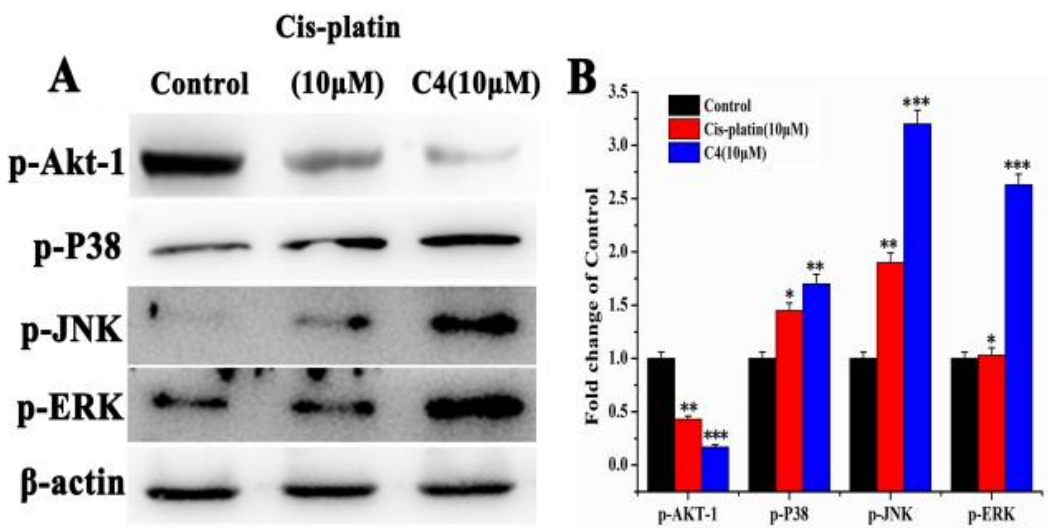

Figure S12 A western blot analysis of Akt1/2 and P38, **B** analysis of the expression percentage level of Akt1/2 and P38; mean ± SD (n= 3):(*) $p < 0.05$, (**) $p < 0.01$,(***) $p < 0.001$.

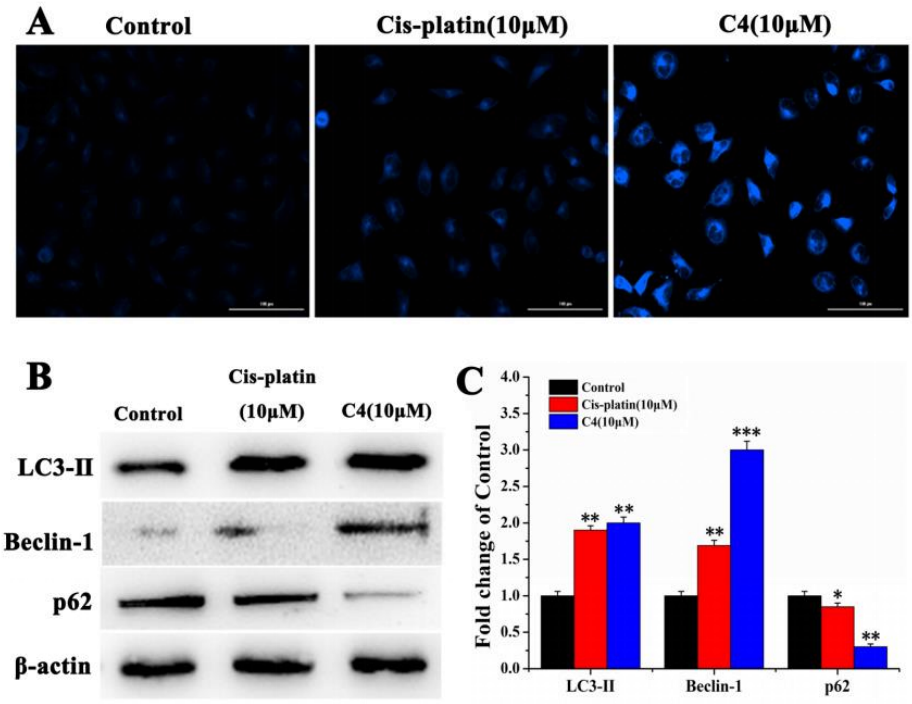

Figure S13 A Morphological analysis of the induction of autophagy after treated with In(III) complex C4 and Cis-platin, **B** Western blot analysis of the expression level of LC3-II, Beclin-1 and P62, relative to control, **C** Graphical presentation of the percentage expression level of LC3-II, Beclin-1 and P62; mean ± SD (n= 3): (*)$p < 0.05$, (**) $p < 0.01$, (***) $p < 0.001$.

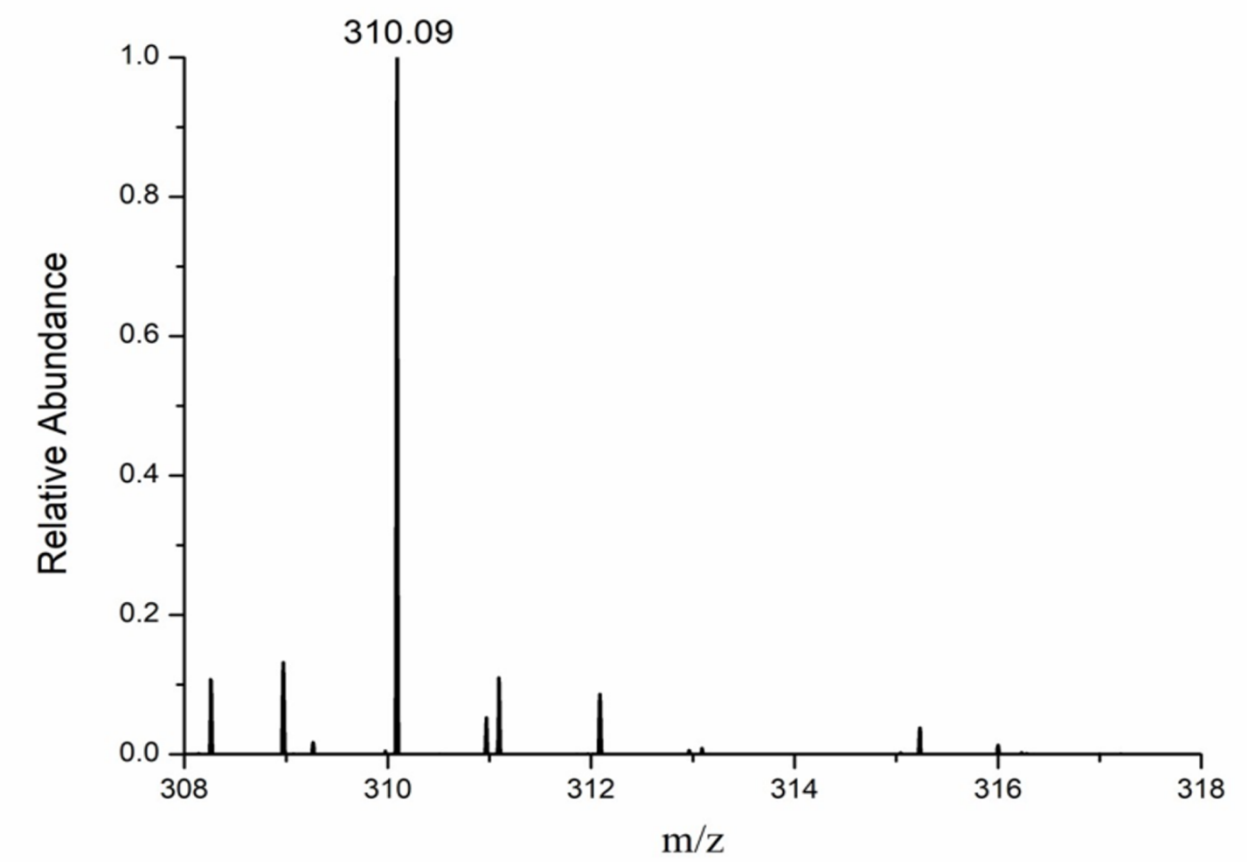

Figure S14 ESI-mass spectrum of the L1 showing an intense signal at m/z= 310.09 for $[M+H]^+$.

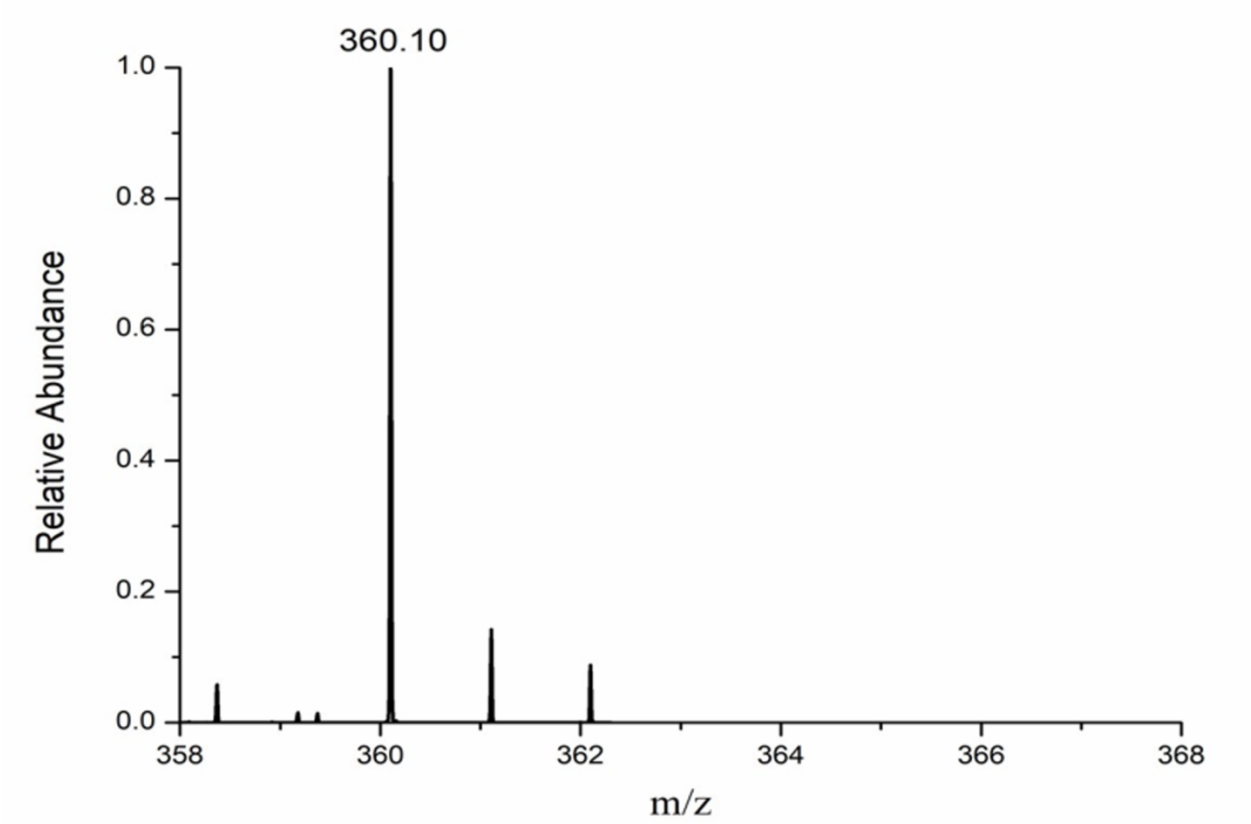

Figure S15 ESI-mass spectrum of the L2 showing an intense signal at m/z=360.10 for $[M+Na]^+$.

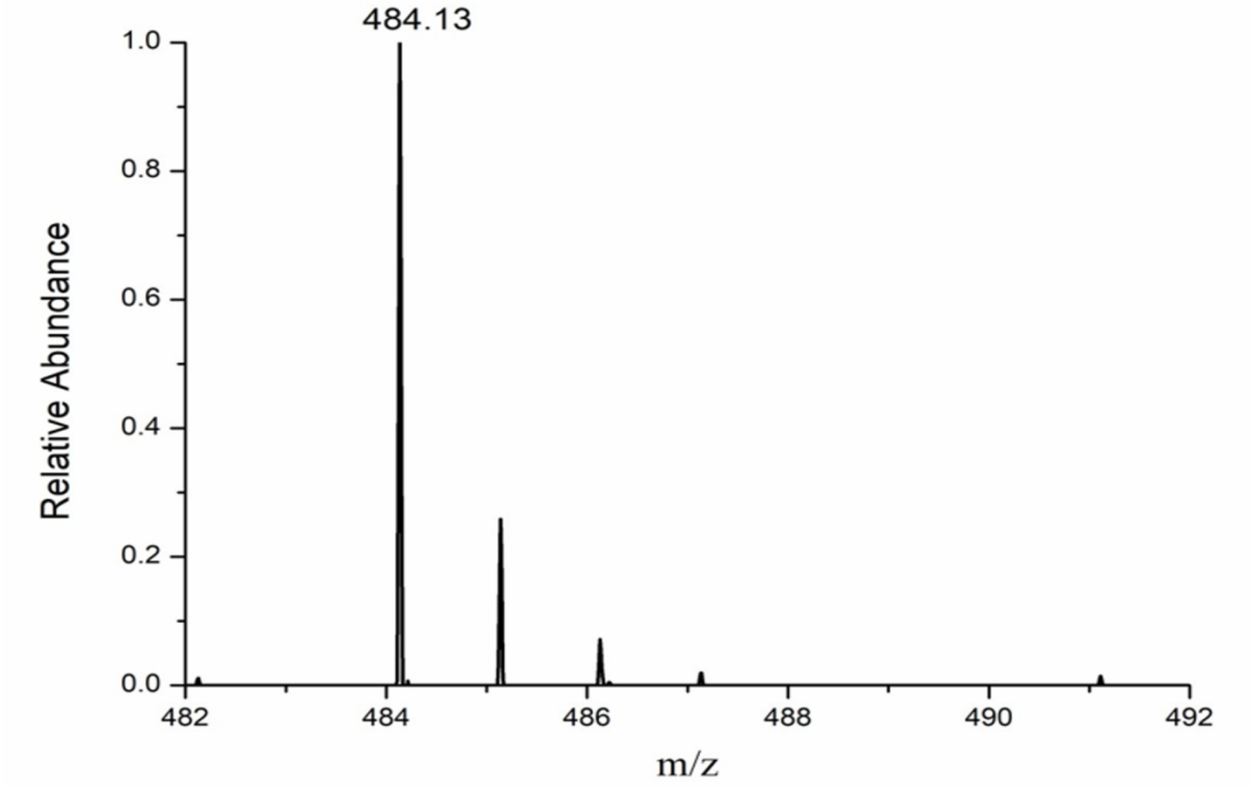

Figure S16 ESI-mass spectrum of the L3 showing an intense signal at m/z=484.13 for $[M+Na]^+$.

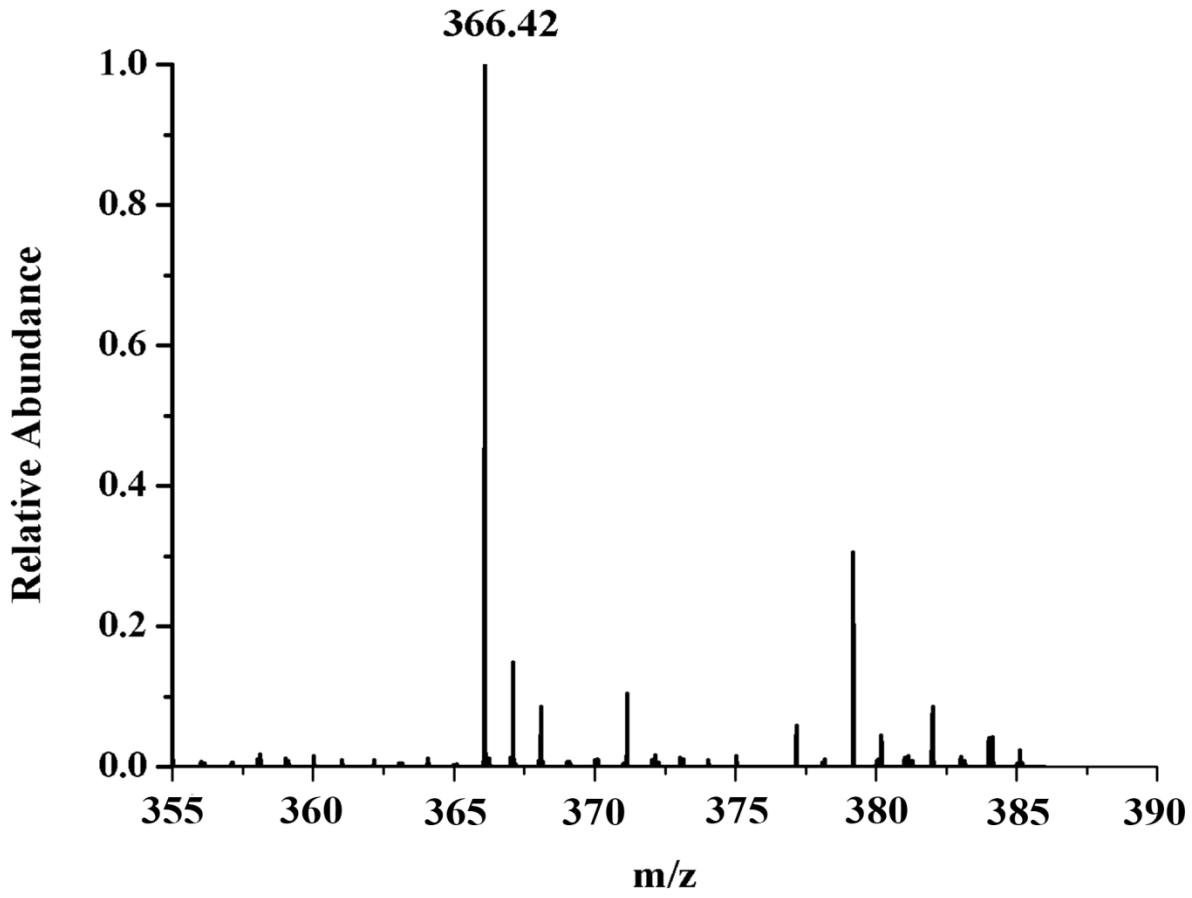

Figure S17 ESI-mass spectrum of the L4 showing an intense signal at m/z=366.42 for $[M+H]^+$.

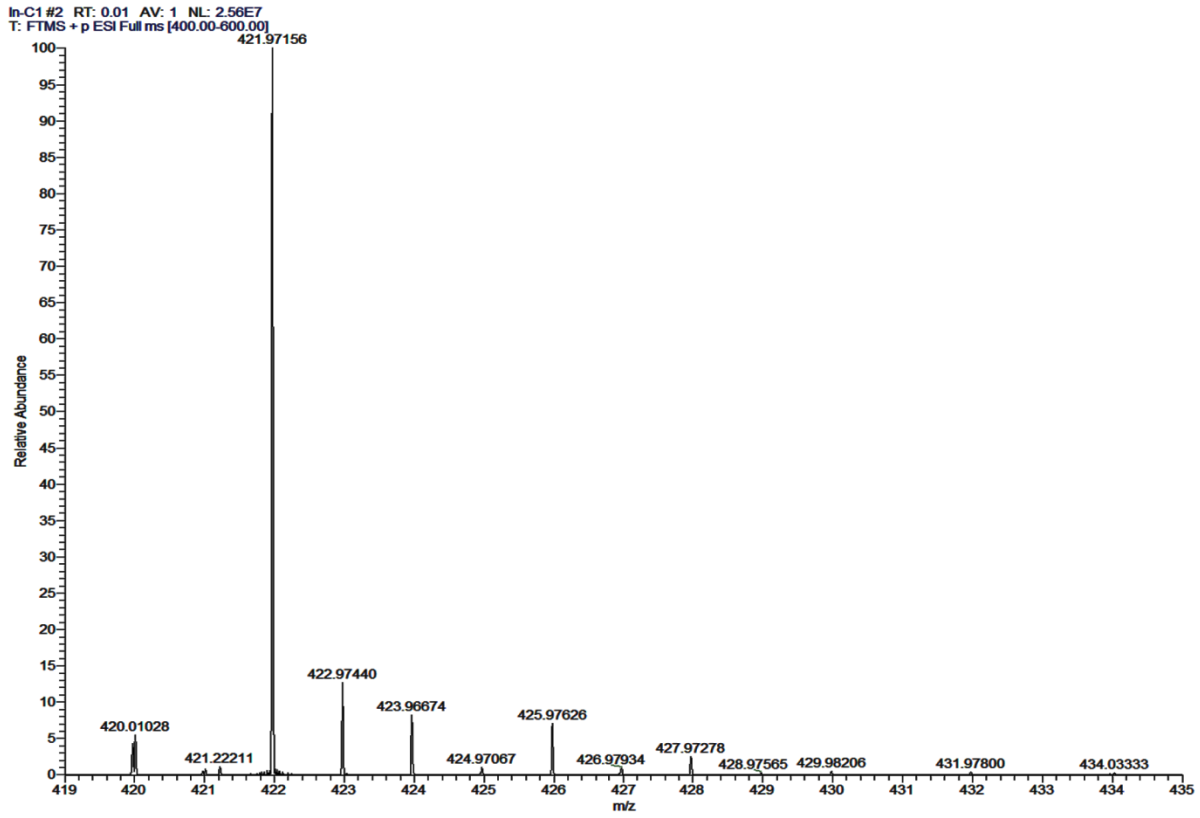

Figure S18 ESI-mass spectrum of the C1 showing an intense signal at m/z=421.97 for $[M -2Cl]^{+}$.

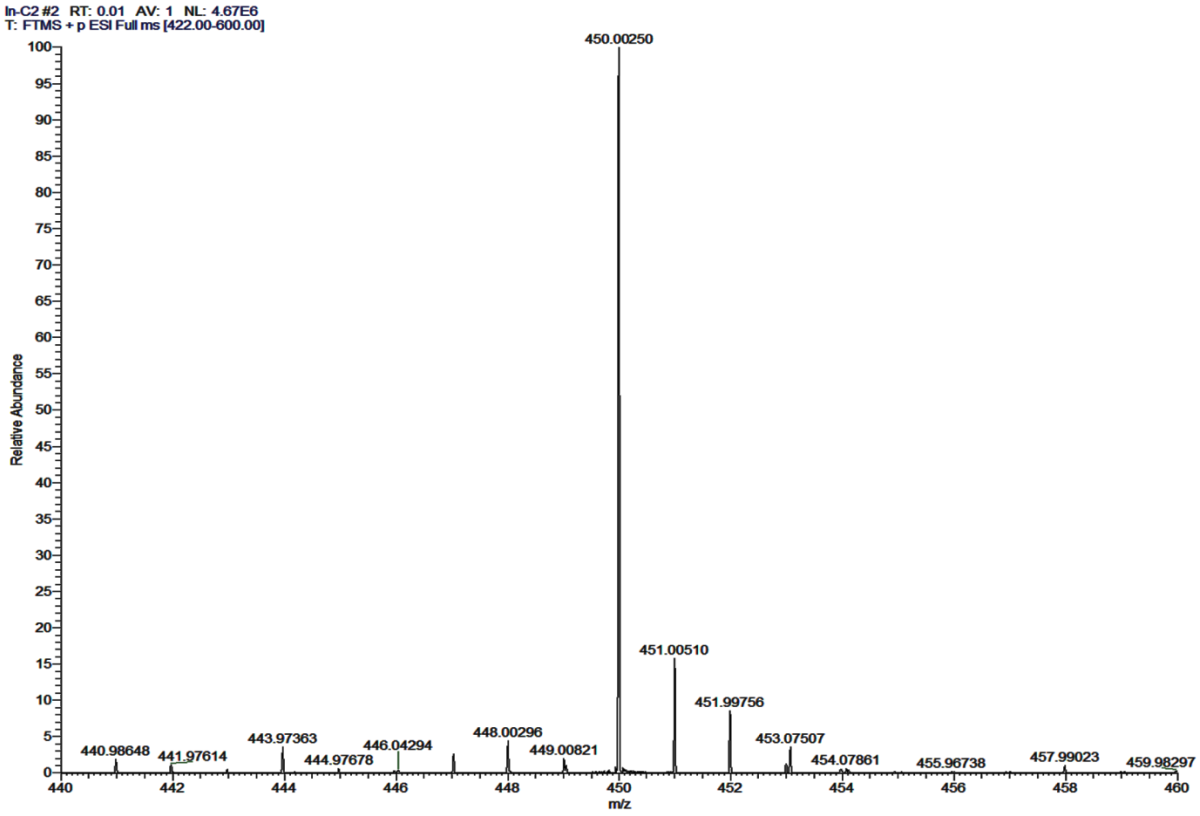

Figure S19 ESI-mass spectrum of the C2 showing an intense signal at m/z =450.00 for **[**M-2Cl]$^{+}$.

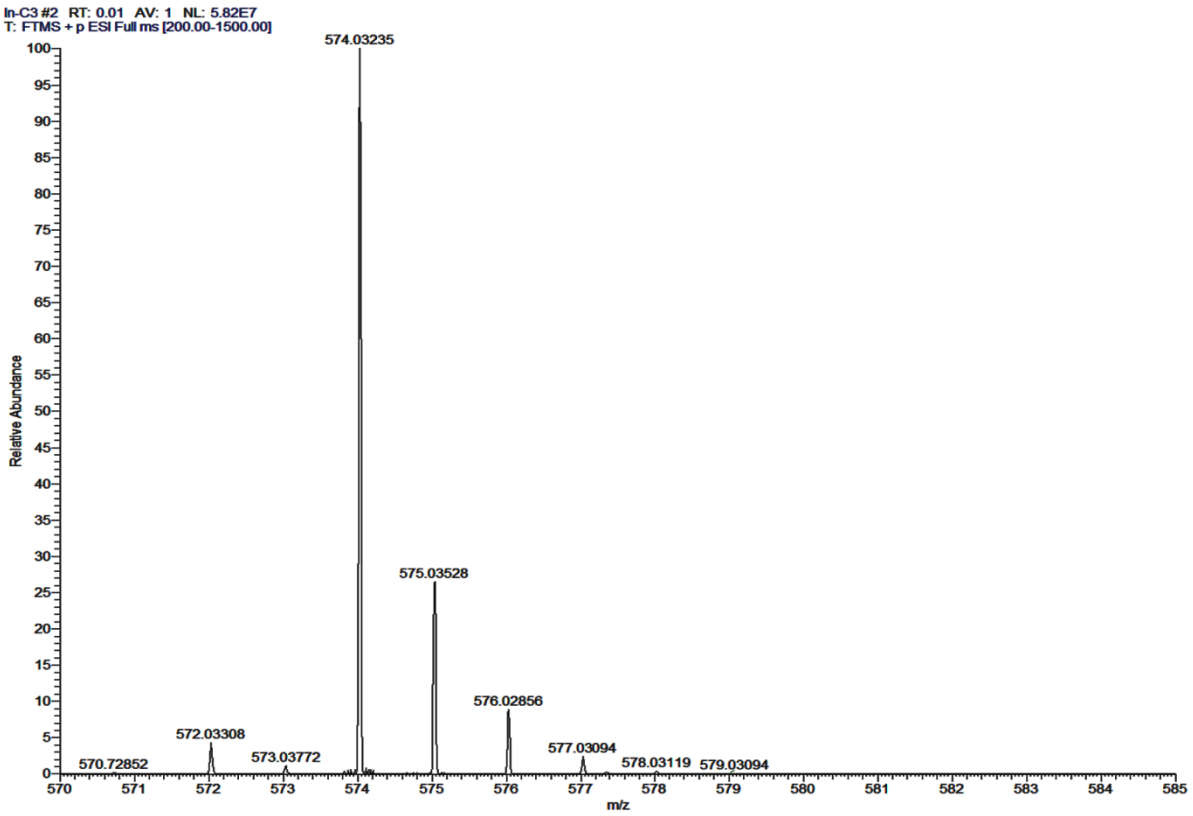

Figure S20 ESI-mass spectrum of the C3 showing an intense signal at m/z =574.03 for $[M - Cl]^+$.

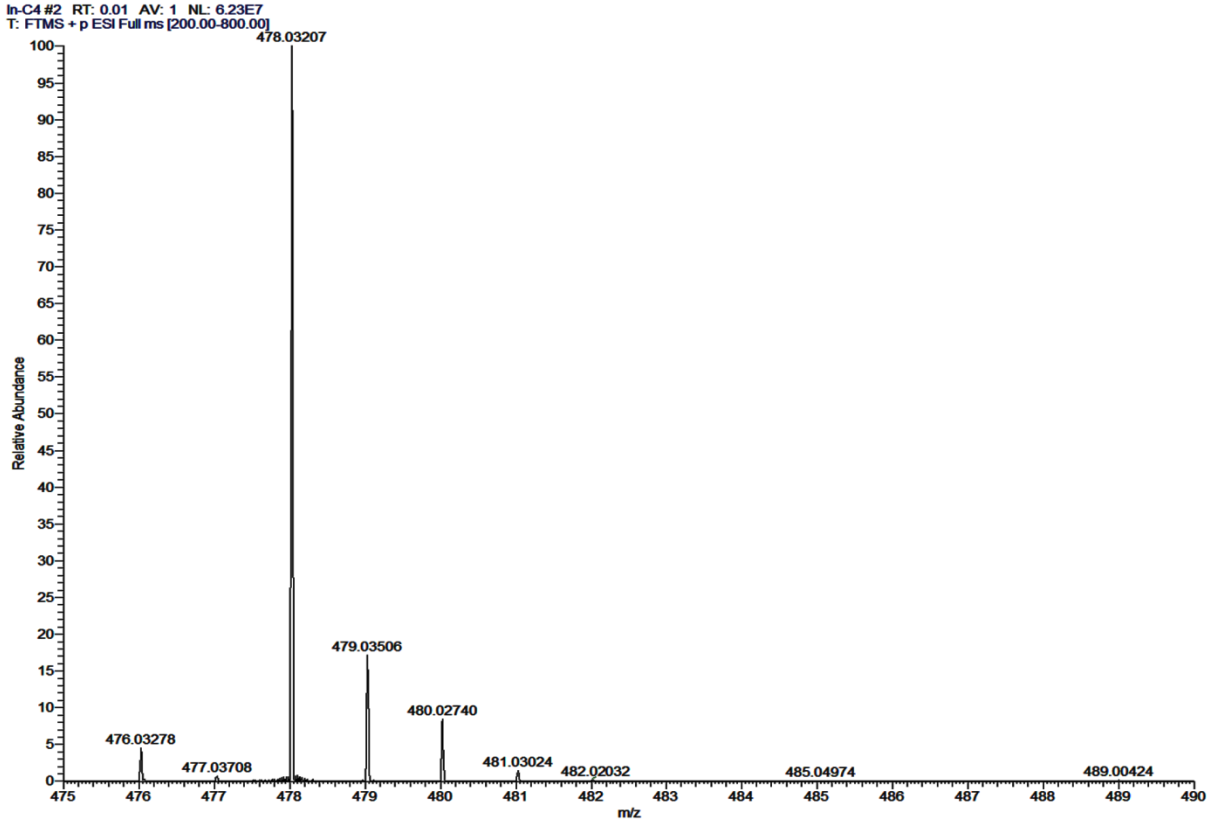

Figure S21 ESI-mass spectrum of the C4 showing an intense signal at m/z=478.03 for $[M\text{-}CH_3OH\text{-}2Cl]^+$.

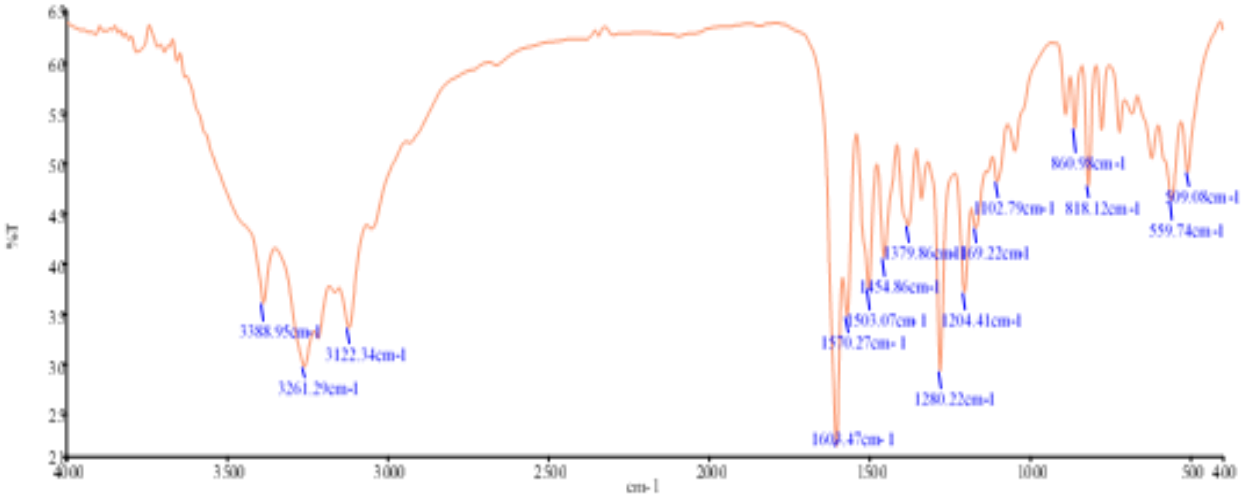

Figure S22 IR spectra of L1

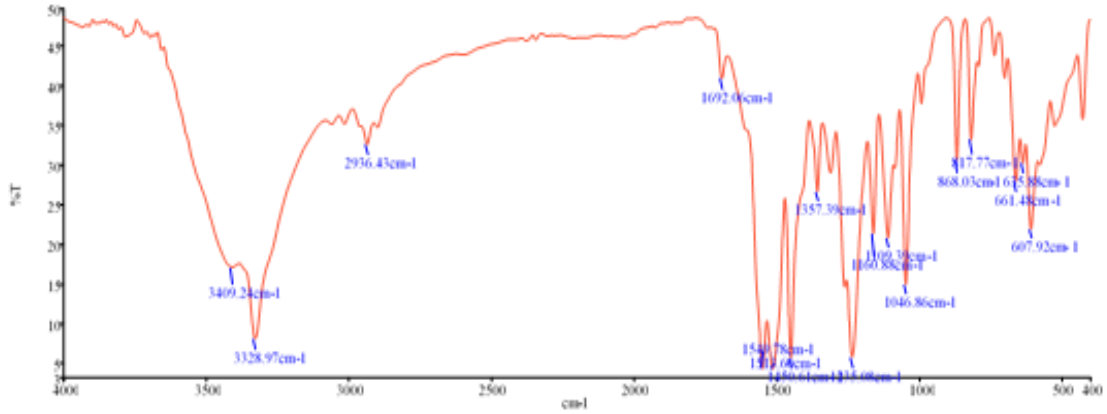

Figure S23 IR spectra of L2

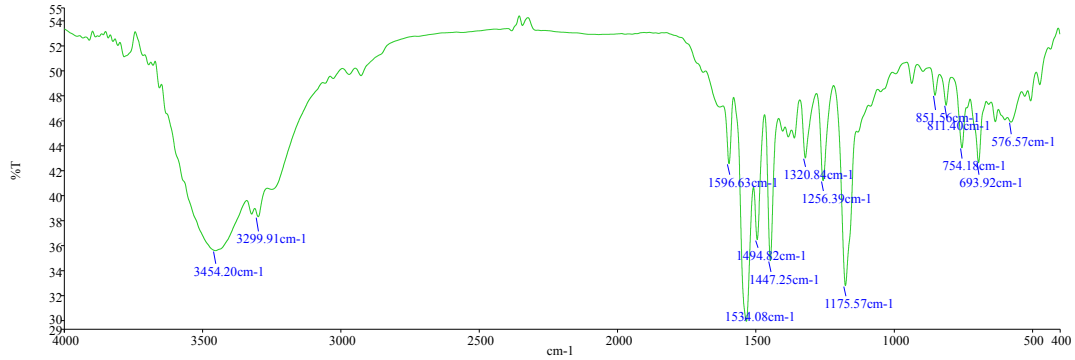

Figure S24 IR spectra of L3

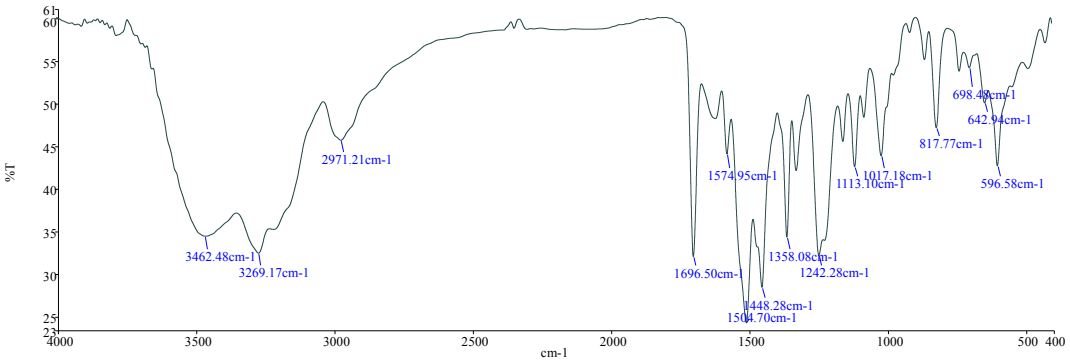

Figure S25 IR spectra of L4

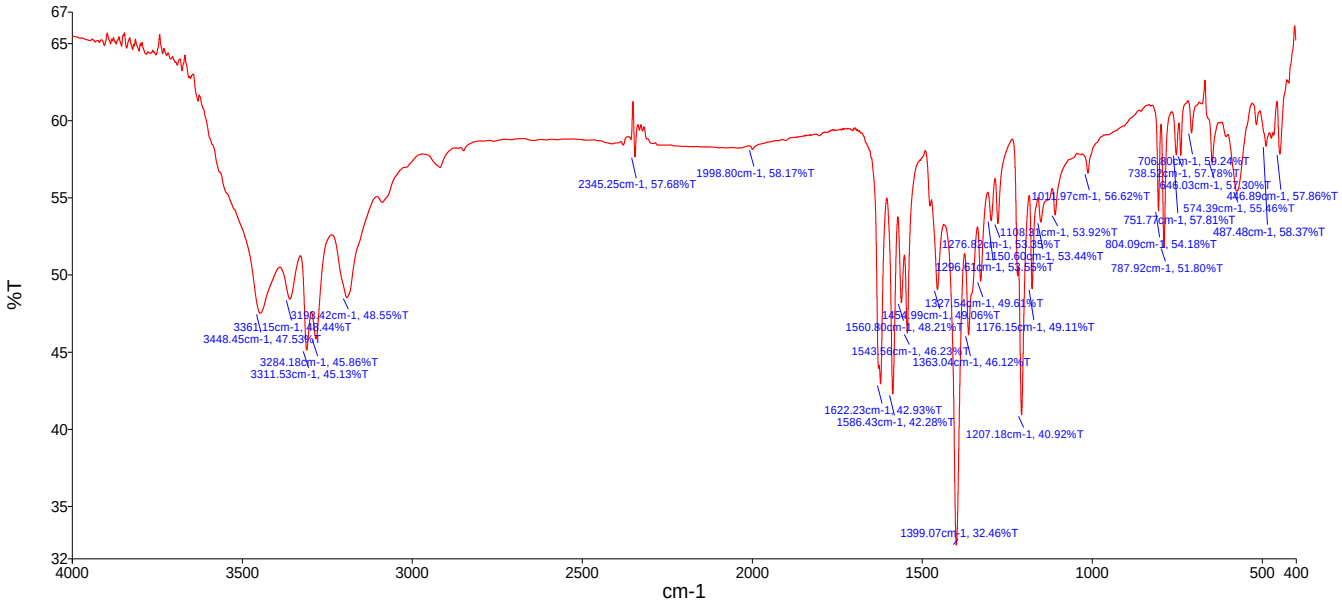

Figure S26 IR spectrum of C1

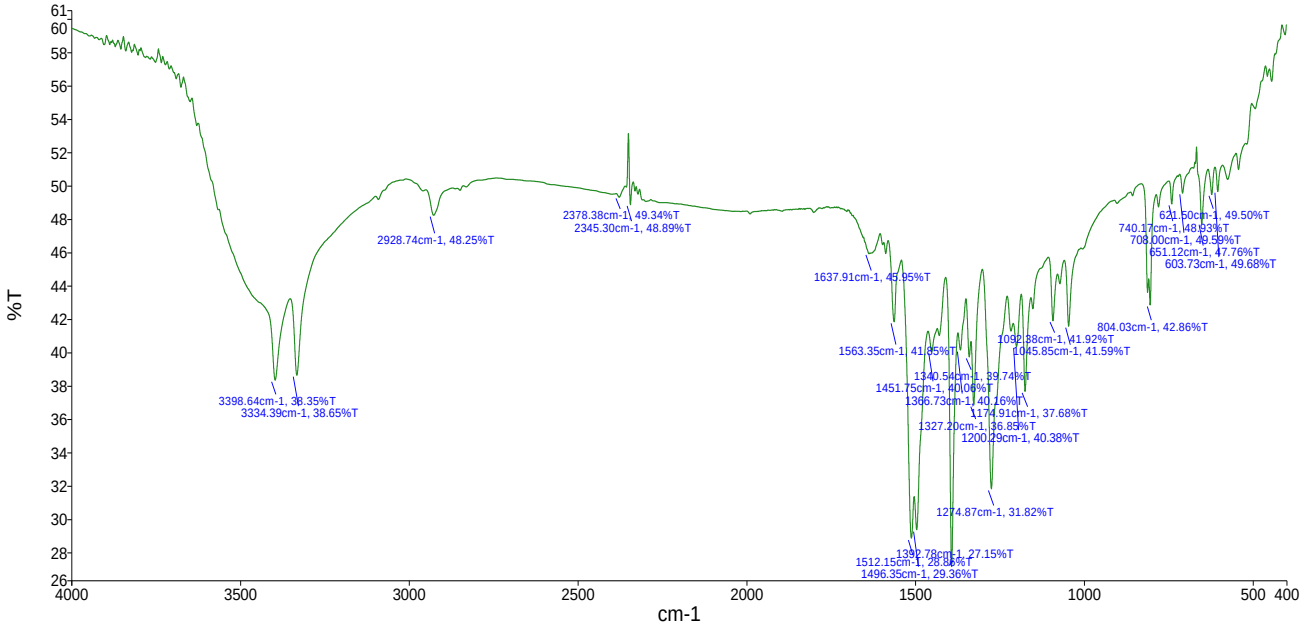

Figure S27 IR spectrum of C2

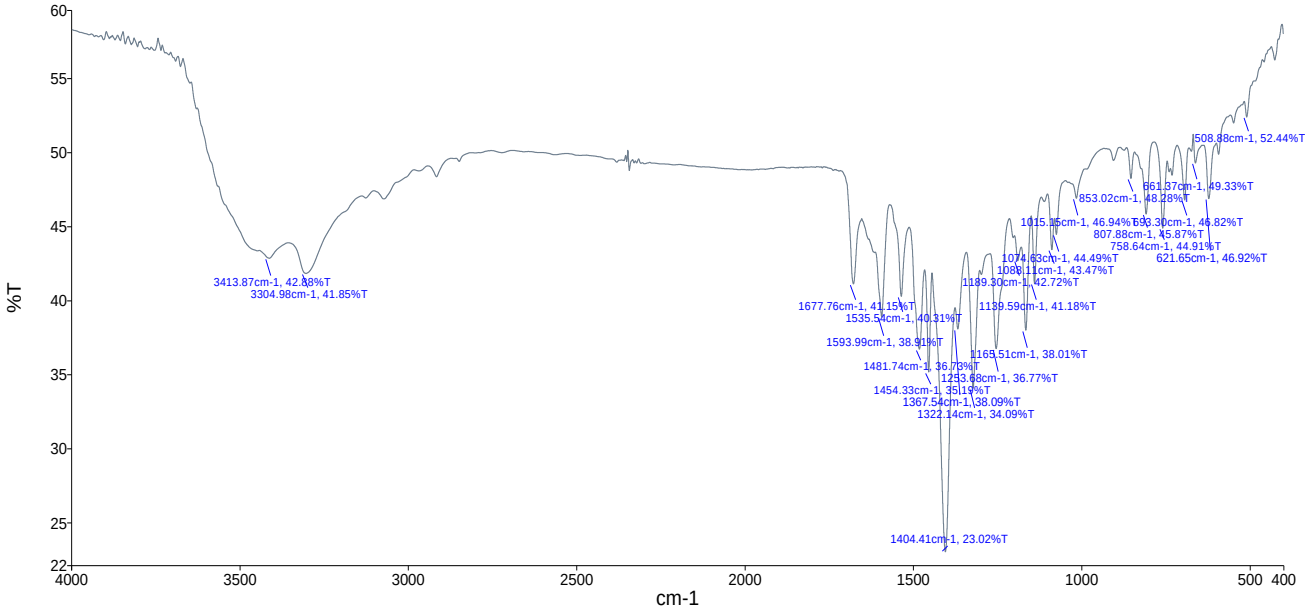

Figure S28 IR spectrum of C3

Figure S29 IR spectrum of C4

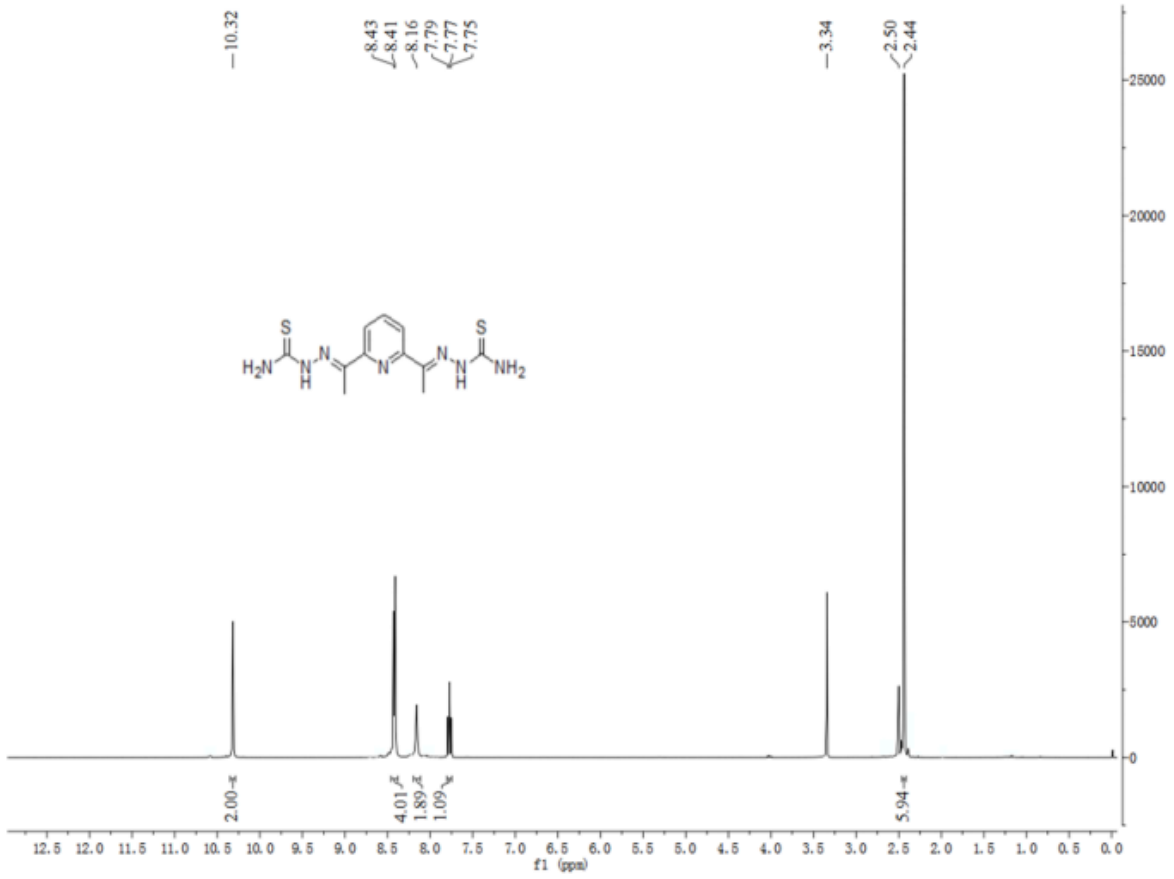

Figure S30 ^{1}H-NMR spectrum of Ligand 1

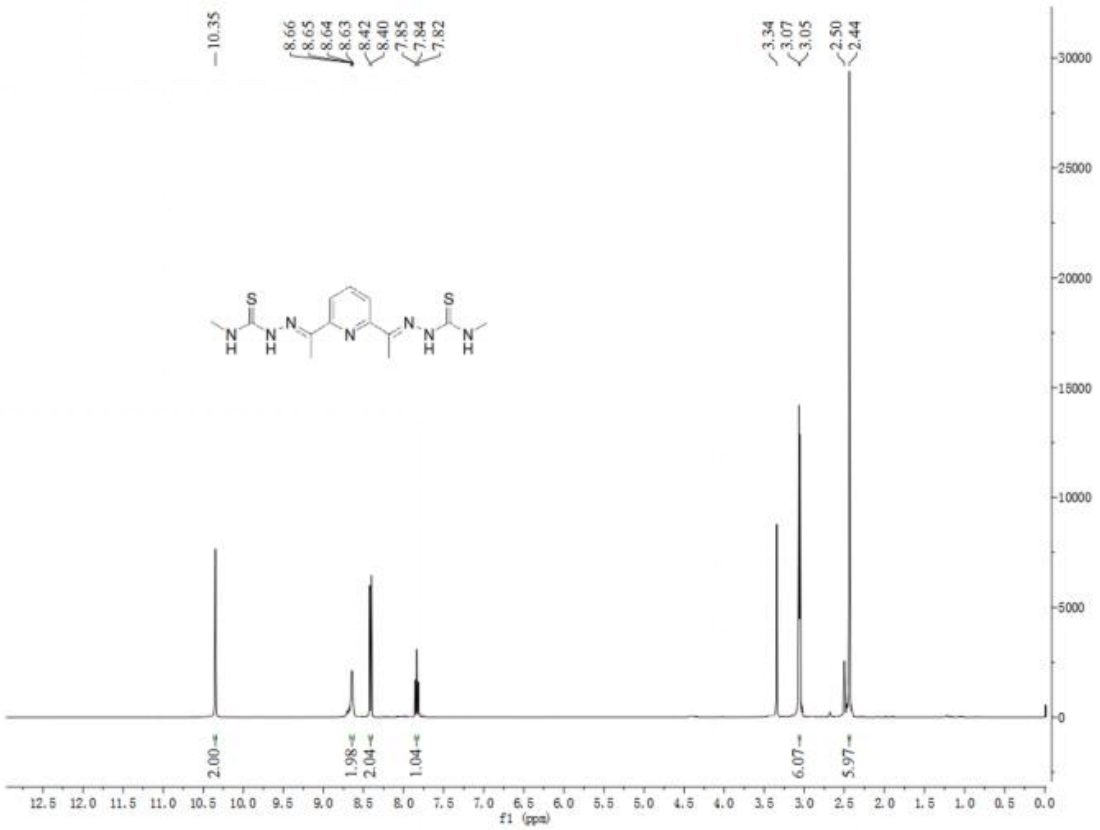

Figure S31 ^{1}H-NMR spectrum of Ligand 2

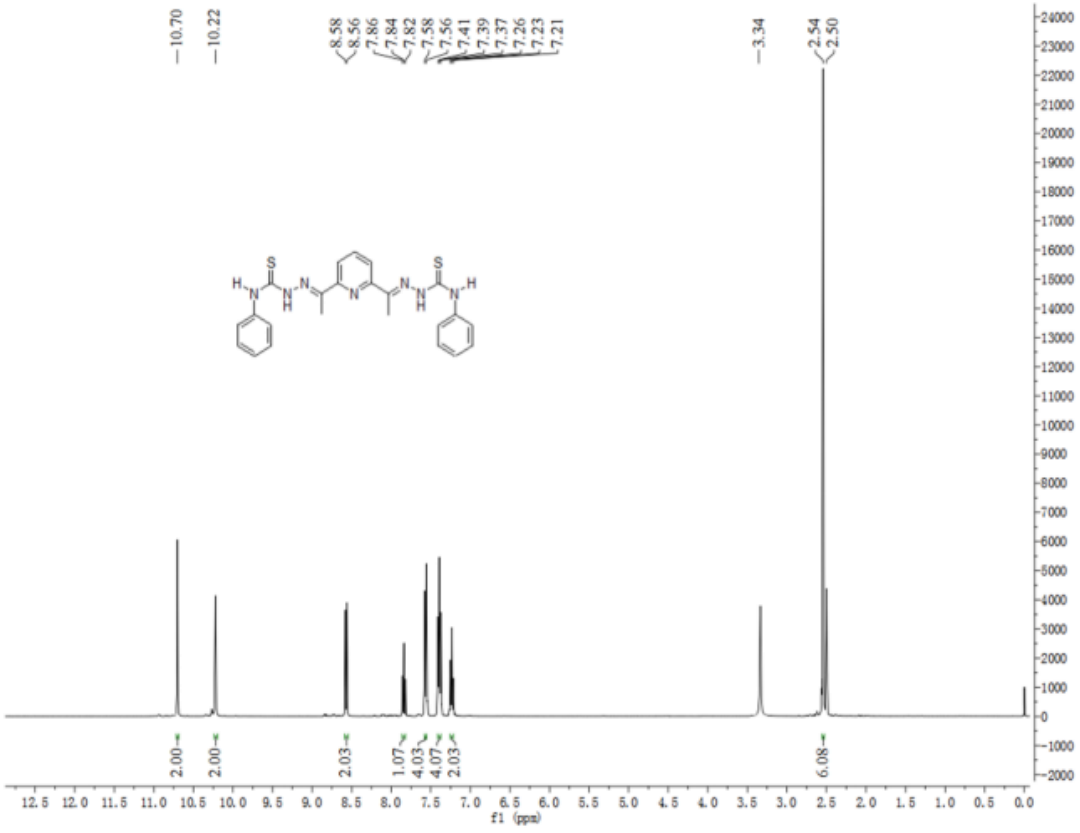

Figure S32 ^{1}H-NMR spectrum of Ligand 3

Figure S33 ^{1}H-NMR spectrum of Ligand 4